The role of sp-hybridized atoms in carbon ferromagnetism: a spin-polarized density functional theory calculation

2010 J. Phys.: Condens. Matter 22 046001

(http://iopscience.iop.org/0953-8984/22/4/046001)

IOP Publishing Journal of Physics: Condensed Matter

J. Phys.: Condens. Matter **22** (2010) 046001 (7pp) doi:10.1088/0953-8984/22/4/046001

The role of sp-hybridized atoms in carbon ferromagnetism: a spin-polarized density functional theory calculation

X F Fan[1], L Liu[1,3], R Q Wu[2], G W Peng[2], H M Fan[2], Y P Feng[2], J-L Kuo[1] and Z X Shen[1]

[1] School of Physical and Mathematical Sciences, Nanyang Technological University, 637616, Singapore

[2] Physics Department, Blk. S12, Faculty of Science, National University of Singapore, 2 Science Drive 3, 117542, Singapore

E-mail: LiuLei@ntu.edu.sg

Received 6 October 2009, in final form 9 November 2009
Published 5 January 2010
Online at stacks.iop.org/JPhysCM/22/046001

Abstract

We address the room-temperature (RT) carbon ferromagnetism by considering the magnetic states of low-dimensional carbons linked by sp-hybridized carbon atoms. Based on the spin-polarized density functional theory calculations, we find that the sp* orbitals of carbon atoms can bring magnetic moments into different carbon allotropes which may eventually give rise to the long-range ferromagnetic ordering at room temperature through an indirect carrier-mediated coupling mechanism. The fact that this indirect coupling is Fermi-level-dependent predicts that the individual magnetism of diverse carbon materials is governed by their chemical environments. This mechanism may help to illuminate the RT magnetic properties of carbon-based materials and to explore the new magnetic applications of carbon materials.

(Some figures in this article are in colour only in the electronic version)

1. Introduction

Ferromagnetism, as is well known, usually has its place in materials with the transition metal elements which possess unpaired d or f electrons [1]. These unpaired electrons can form the local magnetic moments and the coupling between them may result in the collective magnetism. For example, in the RT dilute magnetic semiconductors [2–4], it is expected that the local magnetic moments from the transition metal can be coupled together by the medium carriers (hole or electron) from the semiconductor host. While RT ferromagnetism was routinely recognized as the property of materials containing heavy metallic elements [1], a fundamental question of whether RT ferromagnetism exists in purely light-element materials arises naturally. In the 1980s, the unconventional metal-free ferromagnetism was first seen in pure organic compounds [5, 6]. However, the Curie temperature is just very low, typically much lower than liquid nitrogen temperature, due to the very weak intermolecular ferromagnetic interaction. Therefore, the recent discovery of room-temperature ferromagnetism in carbon has attracted a great deal of attention from the scientific community [7–9].

So far, many experiments have been carried out to study the high-temperature ferromagnetic behaviors in different forms of carbon materials [8, 10–22]. For example, in 2003, Esquinzai *et al* have reported that highly oriented pyrolytic graphite samples bombarded with protons show RT ferromagnetic ordering [14]. In 2004, carbon foam, a spongy form of carbon, was found to have strong but temporary ferromagnetism at room temperature [16]. In 2005, nitrogen- and carbon-irradiated nanosized diamond particles were also found to have RT ferromagnetic hysteretic behavior [18]. In 2009, RT ferromagnetism was reported in graphene material prepared from graphene oxide [21]. While the discovery of RT carbon magnets may be a breakthrough in the search for metal-free magnetic materials, the origin of this magnetic behavior remains an open question [21, 23]. A basic issue is

[3] Author to whom any correspondence should be addressed.

whether magnetism in such light-element material is induced by magnetic impurities. This concern could have been removed and that high-temperature ferromagnetism is the intrinsic property of these carbon-based materials seems to be confirmed by the huge efforts in experiments [9, 18–22]. As the expectation of RT carbon ferromagnetism remains, the primary task would be to illuminate its obscure nature.

To date, a number of mechanisms have been proposed to explain the intrinsic ferromagnetism in carbon [24–30], among which the defect-mediated mechanism is frequently referred to and has been the basis of discussion of magnetism in various carbon structures [31–38]. For example, magnetism in graphite could be ascribed to adatoms [32], vacancy– or vacancy–hydrogen complexes [31], or different mono- and di-hydrogenated graphene ribbon edges [39]. Based on these mechanisms, the local magnetic moment seems to exist in the metal-free carbon compounds, but the origin of ferromagnetism is far more ambiguous [31]. It has been speculated that structural defects would generally give rise to localized electronic states, a net magnetic moment, flat bands associated with defects and thus to an increase in the density of states at the Fermi level, and eventually to the development of magnetic ordering [31]. Another plausible explanation is based on the zigzag edges of graphitic ribbons. If the edge states in a graphitic ribbon are terminated differently, such as with one hydrogen atom on one edge and two hydrogen atoms on the other, itinerant ferromagnetism will be realized due to Lieb's theory [31, 39]. Nevertheless, such an ideal alignment of hydrogen atoms is obviously unfavorable in real materials and cannot explain the intrinsic magnetic behavior of carbon in different forms. Indeed, although the defect states may contribute local magnetic moments to carbon materials, it is still not clear whether such defect-induced spins with random and dilute distributions will necessarily possess long-range ferromagnetic ordering spontaneously in real graphite materials, such as when glued together by charge carriers as in dilute magnetic semiconductors. Thus, further study is highly desirable to clarify the coupling mechanism between defect states in graphite.

Moreover, it is interesting to note that the observed magnetization typically occurs in low-dimensional and amorphous carbon, especially following high temperature or ion implantation, such as boron-doped multi-wall carbon nanotubes [40], carbon nanofoam [9, 16], nitrogen-(^{15}N) and carbon-(^{12}C) irradiated nanosized diamond particles [18], microporous carbon [12], proton-irradiated graphite [14, 15, 19, 20] and graphene prepared from graphene oxide [21]. There are still many polymorphs for carbon which are not ferromagnetic such as bulk graphite, lonsdaleite, diamond, carbon fullerene and carbon nanotubes. Up to now, the theoretical analysis of magnetic carbons has been mainly based on the structures of sp^2 or sp^3 coordinated atoms [24–32, 35, 39]. However, in low-dimensional carbon materials, besides the structural defects with sp^2- and sp^3-hybridized atoms, sp-hybridized carbon with two nearest neighbors will also be present, such as in diamond powder and graphite [41], some single-wall or multi-wall carbon nanotubes [42], and the sp-hybridized carbon chains have been reported [43]. The sp-hybridized atoms can even exist naturally in crystalline solids, such as B_4C [44, 45]. However, up to now, little attention has been paid to the role of sp-hybridized atoms in carbon magnetization.

In this work, we aim to explore the possible mechanism of carbon ferromagnetism with the focus on the role of the sp-coordinated atoms in carbon materials. Based on spin-polarized density functional theory (DFT) calculations, we studied the magnetization of sp atoms in different nonmetal systems, including one-dimensional (1D) carbon nanotubes, two-dimensional (2D) graphite layers and three-dimensional (3D) icosahedral boron nanoclusters. Through a careful theoretical study of the magnetic behavior of sp carbon atoms, we expect to cast some light on under what circumstances high-temperature ferromagnetism in carbon systems can be possible, and on finding new magnetic carbon materials for potential applications.

2. Computational methods

In the present work, spin-polarized DFT calculations based on the local density approximation (LDA) and generalized gradient approximation (GGA) [46] were performed using the plane-wave basis VASP code [47, 48]. The projector augmented wave (PAW) method was used to describe the electron–ion interactions. A kinetic energy cutoff of 400 eV and k-point sampling with 0.05 $Å^{-1}$ separation in the Brillouin zone were used. All structures were optimized until the residual forces were smaller than 0.01 eV $Å^{-1}$. The results of our models were confirmed by using the full-potential linearized augmented plane-wave (FLAPW) method as implemented in the WIEN2K code [49].

3. Results and discussion

3.1. The ferromagnetism from defects

Lehtinen *et al* studied the ferromagnetism from bridged adatom defects on a graphite surface [32]. These adatom defects were found to have a magnetic moment of about 0.5 μ_B and the ferromagnetic state was found to be more favorable than the nonmagnetic states (the energy difference is 35 meV). It was found that the ground state of a vacancy in graphite had a magnetic moment of about 1.0 μ_B and the energy difference between magnetic and nonmagnetic states is about 100 meV [31]. These calculated results seem to show ferromagnetism of carbon materials may originate from defects. Although the structural defects may bring the local magnetic moments of conduction electrons or holes into graphite materials, whether such defect-induced spins possess long-range ferromagnetic ordering spontaneously still needs to be examined further in real carbon materials with low defect concentration.

In order to obtain the real antiferromagnetic (AFM) configurations, the hexagonal symmetry of the graphene/graphite lattice has to be considered as building the supercell models with defects. Based on the Heisenberg model with nearest-neighbor exchange interactions, we construct the supercells with two vacancies or two bridged adatoms. As an example,

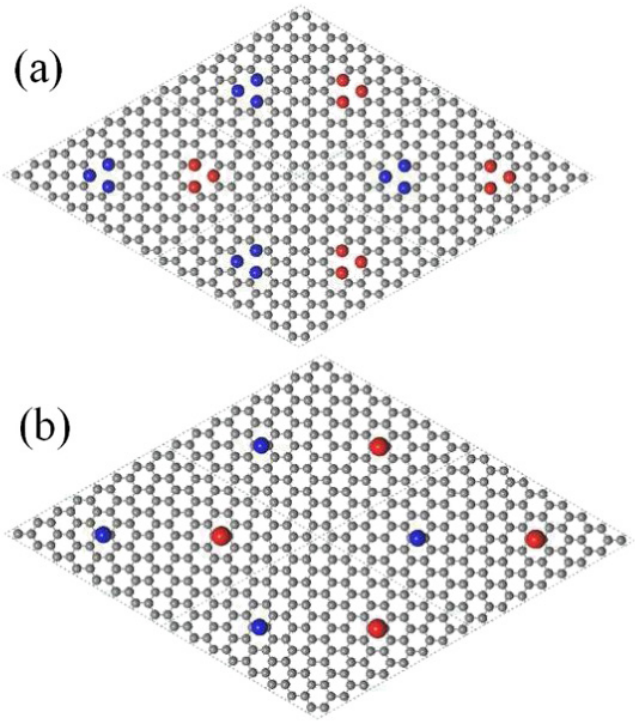

Figure 1. The nearest-neighbor AFM configurations of 8 × 8 supercell of graphene with defects of vacancies (a) and bridged adatoms (b).

the nearest-neighbor AFM configuration in the 8 × 8 supercell with two defects is shown in figure 1. By calculating the energy difference between ferromagnetic (FM) and AFM configurations, the coupling of two defects is found to decrease quickly as their interdistance increases. In the 8 × 8 supercell, the inter-defect distance is about 11.4 Å and the defect concentration is about 1.56%. As their energy differences are very small (1.0 meV for vacancy and 1.8 meV for bridged adatom), the coupling can be almost ignored. This implies that the spin moments reside locally in the lattice and there is no long-range magnetic coupling between them. Although such structural defects will shift the Fermi level and free itinerant states in graphite, they have no capability to spin-polarize these itinerant carriers to form the collective ferromagnetic ordering.

3.2. The sp-hybridized atoms in carbon-based nanomaterials

As the basis of life, carbon is a unique element that bonds to itself through diamond-like sp^3, graphite-like sp^2 and sp hybridization in a variety of polymorphs. So far, the theoretical works on magnetic carbons have been mainly focused on the structures of sp^2 or sp^3 coordinated atoms, while few has been carried out on the role of sp-hybridized atoms in the magnetization of carbon. As natural impurities of sp-hybridized carbons typically present in diamond powder and graphite [41], they also distribute noticeably in nanoscale carbon films [50, 51]. In fact, carbon sp bridge atoms can even exist in crystalline solids, such as B_4C [45]. As the observed magnetization generally occurs in low-dimensional carbon materials which are usually obtained by high-temperature processes or ion implantation, the sp carbon atoms may have an important role in their ferromagnetism and deserve to be studied.

Here, B_4C-based carbon nanocluster models are chosen to illustrate the magnetization of sp carbon atoms between nanoclusters. We first consider the magnetic behavior of the sp carbon atoms embedded in a nanocluster matrix of B_{12} icosahedra forming a B_4C-like structure, where B_{12} icosahedra are connected by the CCC atom chain as shown in figure 2(a). As pure B_4C is a wide-gap semiconductor, to simulate the chemical environment in carbon nanoclusters one N atom is introduced to substitute a chain carbon atom. By replacing N in different positions of the structure, the CCN chain structure is found to be the most stable. Therefore, we can study the magnetic and electronic characteristic of sp carbon based on the configurations with a CCN chain.

In figures 2(c) and (d), the spin-down and spin-up branches of the calculated electronic band structures of $B_{12}C_2N$ are plotted, respectively. They exhibit similar structures except that two spin-down bands near the Fermi level shift up away from their spin-up counterparts by about 0.9 eV at the Γ-point. As only the lower-energy spin-up branch is occupied, the system is half-metallic with a net magnetic moment of about 1.0 μ_B per unit cell. The spin-polarized charge density plotted in figure 2(b) shows the difference of the space distribution between the two spin-polarized bands. It is evident that the spin-polarized charges are mostly localized around the sp carbon atoms and also partially extended to the matrix atoms. As the sp-hybridized orbitals of the bridge carbon atom are along the CCN chain (Z axis), the other p orbitals (p_x and p_y) have to orthogonalize to the sp ones. Under the local crystal field, they will hybridize together and form the new-type orbital sp^*. The major localized sp^* orbitals, if partially occupied, will possess local parallel spins due to Hund's rule. The extended sp^* states are also important, which implies that the local spins may couple to matrix atom orbitals and, through them, form the FM ordering. Moreover, based on Stoner's criterion, the large density of states on the Fermi level is possible to induce the FM ordering.

The stability of ferromagnetic order is evaluated by the energy difference of the FM and AFM configurations, usually based on the doubled unit cells. It is notable that the AFM configuration of a double-sized unit cell is not the true AFM ordering here and should not be employed. To simulate the real nearest-neighbor AFM configuration for the low concentration of local magnetic moments, we construct a $B_{96}C_{22}N_2$ supercell ($2\times2\times2$ of $B_{12}C_2N$ unit cell) with 2 local spins. In figure 3(a), the nearest-neighbor AFM configuration of such a supercell is demonstrated and the N concentration of the supercell $B_{96}C_{22}N_2$ is ∼1.67%. By calculating the energy difference between the nearest-neighbor AFM and FM configurations, the stability of the ferromagnetic ordering in the $B_{96}C_{22}N_2$ supercell is examined. The FM state is found to be more stable with $E_{AFM-FM} = 107.4$ meV, which suggests that the RT ferromagnetic ordering is quite possible. The isosurface of the spin-polarized charge density of $B_{96}C_{22}N_2$ plotted in figure 3(b) indicates further that the coupling between local sp^* orbitals from the CCN chains is mediated by the itinerant states

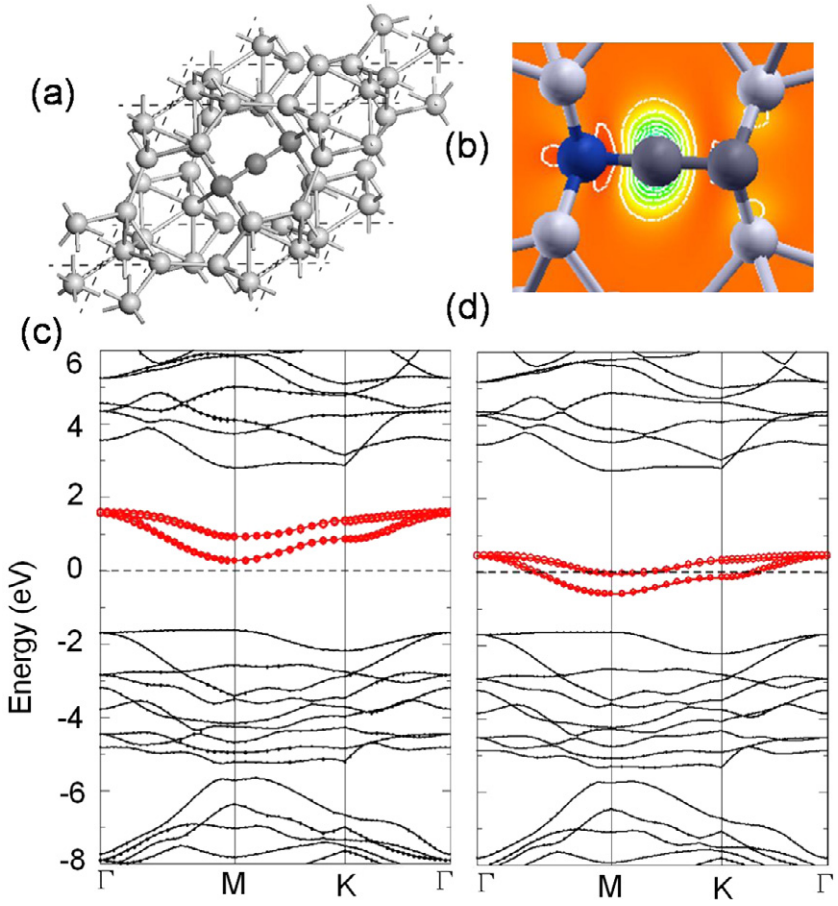

Figure 2. The rhombohedral unit cell of the B_4C structure, consisting of a 12-atom icosahedron (white spheres) and a linear 3-atom chain (black spheres) (a), spin-polarized charge density near the Fermi level in range of 0.6 eV (projected on the (110) plane of the unit cell with 0.1 of total charge as charge unit) with lighter curve indicating the contour plot, (b) the band structure of spin-down channel (c) and of spin-up channel (d) of CCN atom chain connecting boron icosahedra in the B_4C-like structure. The Fermi level is set to zero.

from the matrix boron icosahedra. The p and s orbitals of the matrix boron atoms contribute a minor, but comparable, part to the total density of states (DOS) at the Fermi level, as shown in figure 3(c).

We consider that the magnetic sp atoms are not coupled through the mechanisms of direct-, double- or super-exchange, since the average distance between them is far beyond the nearest-neighbor and next-nearest-neighbor range. The indirect interaction of magnetic carbon atoms actually originates from the coupling between the localized and delocalized electrons. The coupling between sp atoms can be explained by the RKKY mechanism. In figures 2(b) and 3(b), the space distribution of the spin-polarized charge density demonstrates that the small part of charge at the energy positions of sp* orbitals expand to the sites of nearby B atoms. Although the polarized charge on other B atoms is too small to show in the charge unit scale of figures 2(b) and 3(b), the spin density of states of other B atoms in figure 3(c) exhibit clearly the spin-polarized charges of these atoms. This means these itinerant electrons can be coupled with the sp* orbitals from center atoms. Since the concentration of the itinerant electrons from the B icosahedra is rather low as shown in figure 3(c), it is deduced that the ferromagnetic coupling of the sp* local spins can be obtained by the RKKY mechanism [52].

With the RKKY interaction, the carrier-mediated ferromagnetism can be revealed by the Hamiltonian $H_{\mathrm{RKKY}} = \sum_{i,j} J(r_{ij}) S_i \cdot S_j$, where r_{ij} is the separation between two local moments of S_i and S_j [53, 54]. In H_{RKKY}, the exchange integral $J(r_{ij})$ within the free-electron approximation is given by $J(R) \sim F(2k_{\mathrm{F}}R)$, where $k_{\mathrm{F}} = (2/3\pi^2 n_{\mathrm{c}})^{1/3}$ is the Fermi wave vector, $F(x) = (x\cos x - \sin x)/x^4$, and n_{c} is the carrier density. The k_{F} dependence of the RKKY range function implicates that the sign and magnitude of the magnetic coupling between the local sp* spins will rely on the carrier density if the concentration of the magnetic sp atoms is fixed. The band-filling dependence of the energy difference $E_{\mathrm{AFM-FM}}$ is calculated by changing the electron number in the unit cell. The result is plotted in figure 3(d). For the $B_{96}C_{22}N_2$ supercell, sp* orbitals are half-occupied by two electrons. Upon band-filling, the maximum value of $E_{\mathrm{AFM-FM}}$ occurs for about 1.5 electrons per cell. After that, the energy difference will decrease gradually with increasing electron numbers and eventually becomes AFM-negative. Obviously, the band-filling decides the number of free carriers in the modeled structures and limits the local magnetic moments there as well. That means below half-filling of the sp* bands the localized magnetic moments will reduce monotonically with the lowering of Fermi level. However, the sort of oscillation dependence of the magnetic coupling mag-

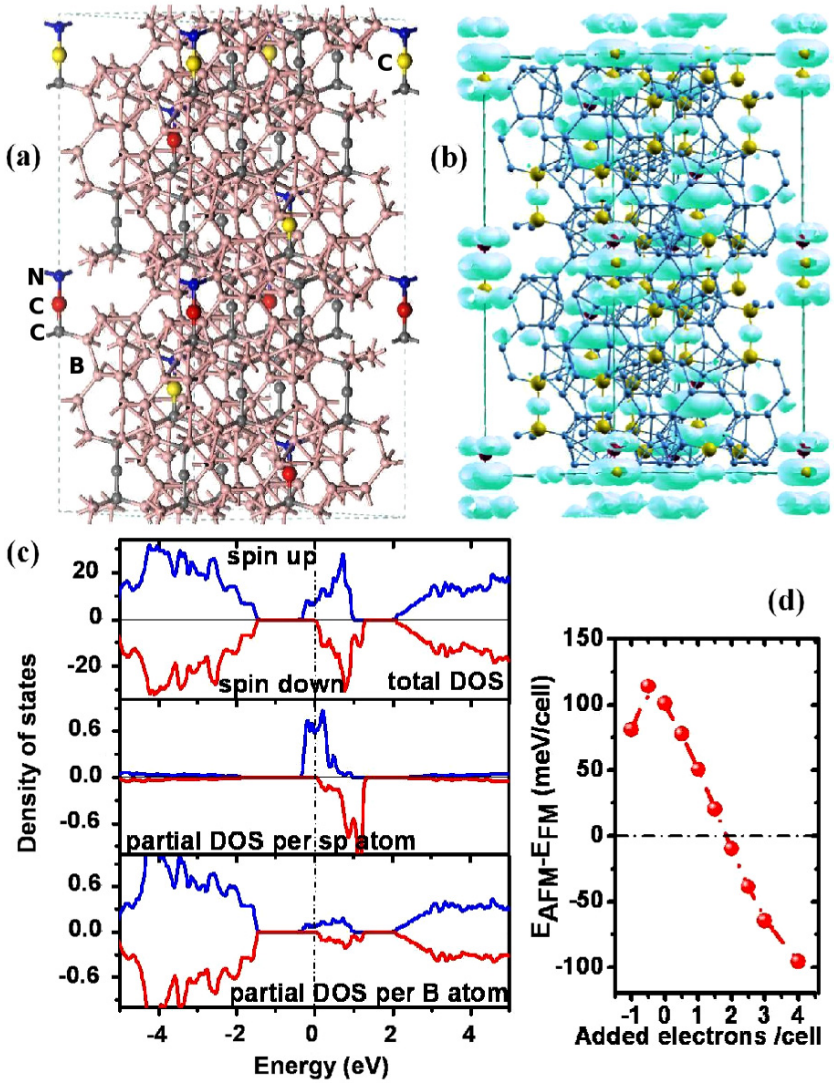

Figure 3. The nearest-neighbor AFM configuration (blue sphere is for N, red, orange and gray sphere are for C and pink is for B) (a) of the $B_{96}C_{22}N_2$ supercell, isosurface of spin polarized charge density near the Fermi level (in range of 0.7 eV with 0.05 of total density as charge unit) (b) and the calculated spin density (c) of the $B_{96}C_{22}N_2$ with FM configuration, and the band filling dependence of the energy difference of $E_{\mathrm{AFM-FM}}$. The Fermi level is set to zero.

nitude on the band-filling level characterizes the RKKY mechanism of the ferromagnetic ordering in the sp carbon materials.

3.3. The sp-hybridized atoms in carbon nanotubes

As sp carbon atoms can bring magnetic states into nanocluster matrices with the long-range FM ordering, it is reasonable to believe that something similar can happen in the curved graphene systems as well. Therefore, we study further the magnetic behavior of sp-atom-connected carbon nanotubes and find that the sp carbon atoms generally carry the local spin moments, whatever the style of the carbon nanotubes chosen.

Without losing generality, we construct a structure of two zigzag (5, 0) carbon nanotubes connected by sp carbon atoms on every fourth zigzag carbon ring as shown in figure 4(a), where the concentration and the inter-atom distance of sp carbons are 1.25% and 8.5 Å, respectively. The magnetic state is found to be the ground state and its spin-resolved density of states is plotted in figure 4(b). While the DOS of matrix carbon atoms keep the same profile in different spin channels, the bands of sp* orbitals split remarkably near the Fermi level. This one-dimensional (1D) system is metallic with a net magnetic moment of about 1.0 μ_{B} per sp atom. The spin-polarized charge density near the Fermi level of the sp carbon linked (5, 0) nanotubes is plotted in figure 4(c), which shows that the spin density is mainly localized around the sp carbon atoms and also extended to the surrounding tube atoms. The FM state is energetically favorable, with $E_{\mathrm{AFM-FM}}$ of 25.0 meV. This indicates that the long-range FM coupling of sp* spins can be mediated by charge carries from curved graphenes.

Considering the indirect coupling nature of the carrier-mediated sp carbon atoms, the room-temperature FM ordering of curved graphene layers can be realized if the Fermi level of the system is tuned properly. As the energy levels of sp* orbitals reside apropos between those of valence π orbitals

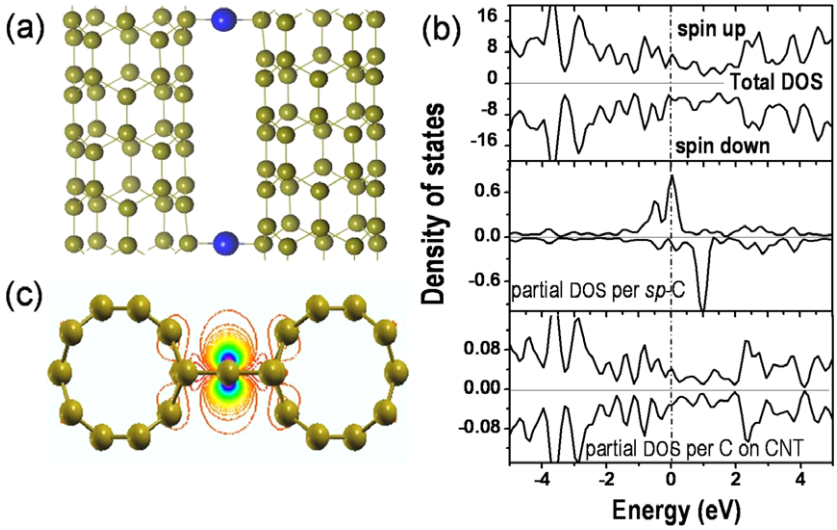

Figure 4. The model structure of (5, 0) carbon nanotubes connected by sp carbon atoms in a supercell with 81 carbon atoms (a), the calculated spin density (b) and spin-polarized charge density near the Fermi level in the range of 0.6 eV (projected on the (001) plane of the unit cell with 0.05 of total charge as the charge unit) (c) of the model structure. The Fermi level is set to zero.

and conduction anti-π orbitals of sp^2 carbon, the sp carbon atoms will generally be partially populated in the sp^2 graphene systems. Our calculations confirm that this is true for both carbon nanotubes and graphene layers as long as they are connected by sp carbon atoms. For the case of three-dimensional carbon matrices with the σ-type sp^3 bonding, as their energy levels of σ and anti-σ orbitals are farther apart than those of π and anti-π orbitals, the sp^*-orbitals will stay within the gap of sp^3 orbitals in the system and be filled partially by electrons as presented in the above $B_{12}C_2N$ model. Accordingly, it should be general that sp carbon atoms induce magnetic states in different carbon matrices.

4. Summary

From the above discussion, we can see that sp^* orbitals of carbon atoms are unusual. Unlike those of π- and σ-bondings in sp^2/sp^3 systems [55], they possess both localized orbitals and itinerant states. As a result, sp carbon atoms with partially populated sp^* orbitals are intrinsically magnetic and can contribute polarized spins. In this case, sp carbon atoms play a similar role as magnetic metal ions in dilute magnetic semiconductors, giving rise to localized magnetic moments in the semiconductor matrix. Although it is still not confirmed experimentally whether the observed magnetization of carbon is due to sp carbon atoms, the sp magnetic carbon mechanism does lead a reasonable way towards the RT ferromagnetism in carbon-based materials. Moreover, the indirect coupling mechanism of sp carbon answers clearly why carbon exhibits different, sometimes even transient, magnetic behaviors under certain circumstances. As the concentration of sp atoms and carrier density are sensitive to the local chemical environment of carbon materials, the coupling between them may not always be ferromagnetic and the aging effect may also arise due to the structural instability. Therefore, based on the physical picture of sp carbon, we can explain the high-temperature ferromagnetic phenomena in low dimensionality carbon materials. Furthermore, it could be a novel way of creating nonmetal magnets by introducing sp carbon into different nonmetal systems. The local polarized spins in such nonmetal systems, especially semiconductors, may be potentially useful in the fabrication of spintronics or quantum computing devices.

The prerequisite of intrinsic room-temperature long-range FM ordering in pure carbon materials is the coexistence of magnetic moments and the effective coupling mechanism between them. Although structural defects such as bridged adatoms and vacancies may introduce local spins in carbons, they do not necessarily couple strongly with itinerant states such as π electrons and would lack the long-range coupling. This work demonstrates the important role of sp coupling in carbon ferromagnetism. The carrier-mediated coupling mechanism of sp-hybridized carbon atoms is shown to account for the RT ferromagnetic behaviors of different carbon allotropes.

References

[1] Heisenberg W 1928 *Z. Phys.* **49** 619–36
[2] Ohno H 1998 *Science* **281** 951
[3] Dietl T, Ohno H, Matsukura F, Cibert J and Ferrand D 2000 *Science* **287** 1019
[4] Pearton S J, Abernathy C R, Norton D P, Hebard A F, Park Y D, Boatner L A and Budai J D 2003 *Mater. Sci. Eng.* R **40** 137
[5] Chiarelli R, Noval M A, Rassat A and Tholence J L 1993 *Nature* **147** 363
[6] Rajca A, Wongsriratanakul J and Rajca S 2001 *Science* **294** 1503
[7] Coey J M D, Venkatesan M, Fitzgerald C B, Douvalis A P and Sanders I S 2002 *Nature* **420** 156
[8] Wang X, Liu Z X, Zhang Y L, Li F Y, Yu R C and Jin C Q 2002 *J. Phys.: Condens. Matter* **14** 10265

[9] Service R F 2004 *Science* **304** 42
[10] Schindler K, García N, Esquinazi P and Ohldag H 2008 *Phys. Rev.* B **78** 045433
[11] Kopelevich Y, Esquinazi P, Torres J H S and Moehlecke S 2000 *J. Low Temp. Phys.* **119** 691
[12] Kopelevich Y, da Silva R R, Torres J H S, Penicaud A and Kyotani T 2003 *Phys. Rev.* B **68** 092408
[13] Höhne R and Esquinazi P 2002 *Adv. Mater.* **14** 753
[14] Esquinazi P, Spemann D, Höhne R, Setzer A, Han K-H and Butz T 2003 *Phys. Rev. Lett.* **91** 227201
[15] Han K-H, Spemann D, Esquinazi P, Höhne R, Riede V and Butz T 2003 *Adv. Mater.* **15** 1719
[16] Rode A V, Gamaly E G, Christy A G, Gerald J G F, Hyde S T, Elliman R G, Luther-Davies B, Veinger A I, Androulakis J and Giapintzakis J 2004 *Phys. Rev.* B **70** 054407
[17] Mombrú A W, Pardo H, Faccio R, Lima O F d, Leite E R, Zanelatto G, Lanfredi A J C, Cardoso C A, Luther-Davies B and Araújo-Moreira F M 2005 *Phys. Rev.* B **71** 100404(R)
[18] Talapatra S, Ganesan P G, Kim T, Vajtai R, Huang M, Shima M, Ramanath G, Srivastava D, Deevi S C and Ajayan P M 2005 *Phys. Rev. Lett.* **95** 097201
[19] Barzola-Quiquia J, Esquinazi P, Rothermel M, Spemann D, Butz T and García N 2007 *Phys. Rev.* B **76** 161403(R)
[20] Ohldag H, Tyliszczak T, Höhne R, Spemann D, Esquinazi P, Ungureanu M and Butz T 2007 *Phys. Rev. Lett.* **98** 187204
[21] Wang Y, Huang Y, Song Y, Zhang X, Ma Y, Liang J and Chen Y 2009 *Nano Lett.* **9** 220
[22] Cervenka J, Katsnelson M I and Flipse C F J 2009 *Nat. Phys.* **5** 840
[23] Coey J M D and Sanvito S 2004 *Phys. World* **17** 33
[24] Park N, Yoon M, Berber S, Ihm J, Osawa E and Tománek D 2003 *Phys. Rev. Lett.* **91** 237204
[25] Mattis D C 2005 *Phys. Rev.* B **71** 144424
[26] Ma Y, Foster A S, Krasheninnikov A V and Nieminen R M 2005 *Phys. Rev.* B **72** 205416
[27] Lee H, Son Y-W, Park N, Han S and Yu J 2005 *Phys. Rev.* B **72** 174431
[28] Fernández-Rossier J and Palaciosl J J 2007 *Phys. Rev. Lett.* **99** 177204
[29] Uchoa B, Kotov V N, Peres N M R and Neto A H C 2008 *Phys. Rev. Lett.* **101** 026805
[30] Yazyev O V 2008 *Phys. Rev. Lett.* **101** 037203
[31] Lehtinen P O, Foster A S, Ma Y, Krasheninnikov A V and Nieminen R M 2004 *Phys. Rev. Lett.* **93** 187202
[32] Lehtinen P O, Foster A S, Ayuela A, Krasheninnikov A, Nordlund K and Nieminen R M 2003 *Phys. Rev. Lett.* **91** 017202
[33] Vozmediano M A H, López-Sancho M P, Stauber T and Guinea F 2005 *Phys. Rev.* B **72** 155121
[34] Yazyev O V and Helm L 2007 *Phys. Rev.* B **75** 125408
[35] Zhang Y, Talapatra S, Kar S, Vajtai R, Nayak S K and Ajayan P M 2007 *Phys. Rev. Lett.* **99** 107201
[36] Faccio R, Pardo H, Denis P A, Oeiras R Y, Araújo-Moreira F M, Veríssimo-Alves M and Mombrú A W 2008 *Phys. Rev.* B **77** 035416
[37] Palacios J J, Fernández-Rossier J and Brey L 2008 *Phys. Rev.* B **77** 195428
[38] López-Sancho M P, de Juan F and Vozmediano M A H 2009 *Phys. Rev.* B **79** 075413
[39] Kusakabe K and Maruyama M 2003 *Phys. Rev.* B **67** 092406
[40] Likodimos V, Glenis S and Lin C L 2005 *Phys. Rev.* B **72** 045436
[41] Kudryavtsev Y P, Heimann R B and Evsyukov S E 1996 *J. Mater. Sci.* **31** 5557
[42] Fantini C, Cruz E, Jorio A, Terrones M, Terrones H, Lier G V, Charlier J-C, Dresselhaus M S, Saito R, Kim Y A, Hayashi T, Muramatsu H, Endo M and Pimenta M A 2006 *Phys. Rev.* B **73** 193408
[43] Zhao X, Ando Y, Liu Y, Jinno M and Suzuki T 2003 *Phys. Rev. Lett.* **90** 187401
[44] Mauri F, Vast N and Pickard C J 2001 *Phys. Rev. Lett.* **87** 085506
[45] Werheit H 2006 *J. Phys.: Condens. Matter* **18** 10655
[46] Perdew J P, Burke K and Wang Y 1996 *Phys. Rev.* B **54** 16533
[47] Kresse G and Furthmüller J 1996 *Phys. Rev.* B **54** 11169
[48] Kresse G and Furthmüller J 1996 *Comput. Mater. Sci.* **6** 15
[49] Schwarz K, Blaha P and Madsen G K H 2002 *Comput. Phys. Commun.* **147** 71
[50] Barborini E, Piseri P, Bassi A L, Ferrari A C, Bottani C E and Milani P 1999 *Chem. Phys. Lett.* **300** 633
[51] Lucotti A, Tommasini M, Fazzi D, Zoppo M D, Chalifoux W A, Ferguson M J, Zerbi G and Tykwinski R R 2009 *J. Am. Chem. Soc.* **131** 4239
[52] Ruderman M A and Kittel C 1954 *Phys. Rev.* **96** 99
[53] Dietl T, Haury A and d'Aubigné Y M 1997 *Phys. Rev.* B **55** R3347
[54] Priour J D J and Sarma S D 2006 *Phys. Rev. Lett.* **97** 127201
[55] Veciana J 2001 *p-Electron Magnetism: From Molecules to Magnetic Materials* (Berlin: Springer)